Title
What is MEMS Gyrocompassing? Comparative Analysis of Maytagging and Carouseling

Journal
Journal of Microelectromechanical Systems, 22(6)

ISSN
1057-7157

Authors
Prikhodko, Igor P
Zotov, Sergei A
Trusov, Alexander A
et al.

Publication Date
2013-12-01

DOI
10.1109/jmems.2013.2282936

Peer reviewed

What is MEMS Gyrocompassing? Comparative Analysis of Maytagging and Carouseling

Igor P. Prikhodko, *Member, IEEE*, Sergei A. Zotov, *Member, IEEE*, Alexander A. Trusov, *Member, IEEE*, and Andrei M. Shkel, *Senior Member, IEEE*

***Abstract*— North-finding based on micromachined gyroscopes is an attractive possibility. This paper analyzes north-finding methods and demonstrates a measured 4 mrad standard deviation azimuth uncertainty using an in-house developed vibratory silicon MEMS quadruple mass gyroscope (QMG). We instrumented a vacuum packaged QMG with isotropic Q-factor of 1.2 million and Allan deviation bias instability of 0.2 °/hr for azimuth detection by measuring the earth's rotation. Continuous rotation ("carouseling") produced azimuth datapoints with uncertainty diminishing as the square root of the number of turns. Integration of 100 datapoints with normally distributed errors reduced uncertainty to 4 mrad, beyond the noise of current QMG instrumentation. We also implemented self-calibration methods, including *in-situ* temperature sensing and discrete ±180° turning ("maytagging" or two-point gyrocompassing) as potential alternatives to carouseling. While both mechanizations produced similar azimuth uncertainty, we conclude that carouseling is more advantageous as it is robust to bias, scale-factor, and temperature drifts, although it requires a rotary platform providing continuous rotation. Maytagging, on the other hand, can be implemented using a simple turn table, but requires calibration due to temperature-induced drifts. [2012-0378]**

***Index Terms*— MEMS gyroscope, gyrocompassing, north-finding, azimuth seeking, heading, carouseling, maytagging.**

I. Introduction

NORTH-FINDING with a single digit milliradian (mrad) uncertainty is required for setting the initial orientation in the dead reckoning, targeting, pointing, and inertial guidance [1]. North identification is traditionally accomplished through the use of magnetic field of the Earth; however, there are a number of spatial and temporal distortions in this field due to varying magnetic background, which limit the accuracy of magnetic compasses. Moreover, practical limitations of geodetic, celestial, and GPS-based methods make high performance gyroscopes desirable for true north finding. A method of north-finding based on gyroscopes is commonly referred to as "gyrocompassing." Although commercially available macro-scale fiber optic, ring laser, and quartz hemispherical resonator gyroscopes (with 10^{-4} °/hr bias instability) [2] can be used for precision gyrocompassing, they are not suitable for man-portable and small platform applications [3]. Attempts to miniaturize optical gyroscopes decrease their reliability, especially due to the unpredictable lifetime of compact laser sources (e.g. VCSELs) [4]. MEMS, in contrast, have a number of inherent benefits when used as inertial sensors: they are light-weight, low-power, batch-fabricated, and are potentially capable of high performance operation, given the proper design.

North-finding based on micromachined gyroscopes is an intriguing possibility, but silicon MEMS are yet to establish credibility in the high-precision domain [5]. Gyrocompassing requires repeatable and stable measurements of extremely low angular rates (fractions of the Earth's rate). For instance, a gyroscope's bias error of only 1 °/hr leads to a 100 mrad azimuth uncertainty (at a 45° latitude), which translates to a 9 m location error per each 100 m of dead reckoning or targeting distance. While several groups have reported silicon MEMS gyroscopes with less than 1 °/hr Allan deviation bias instability [6]–[9], north-finding with a single digit mrad error is often assumed unattainable by MEMS technology.

The common approaches to reduce the effect of bias drift on azimuth measurements include "carouseling" [6] and "maytagging" [10], [11]. We propose to tackle the problem of MEMS gyrocompassing by using the recently developed Quadruple Mass Gyroscope (QMG) [12], with the performance enhanced by Quality (Q) factors of 1.2 million, in drive- and sense-modes, and Allan deviation bias instability of 0.2 °/hr [13]. Recently, we have demonstrated an application of the high performance QMG to gyrocompassing and performed a comparative study of carouseling and maytagging approaches [14]. In this paper, we present a more complete account of the gyrocompassing results and bias drift mitigation approaches. As a potential alternative to the common approaches, we have also demonstrated bias drift compensation algorithm for maytagging utilizing the in-situ temperature sensing.

This paper is organized as follows. Section 2 introduces basic gyrocompassing principles. Section 3 presents gyroscope noise analysis and derives sensor requirements. Section 4 reports characterization of the sensor, north-finding setup,

Manuscript received December 15, 2012; revised May 22, 2013; accepted August 5, 2013. Date of publication October 11, 2013; date of current version November 25, 2013. This work was supported in part by the Office of Naval Research and in part by the Naval Surface Warfare Center Dahlgren Division under Grant N00014-09-1-0424 and Grant N00014-11-1-0483. Subject Editor C. Rembe.

I. P. Prikhodko was with the Department of Mechanical and Aerospace Engineering, MicroSystems Laboratory, University of California, Irvine, CA 92697 USA. He is now with Analog Devices Inc., Wilmington, MA 01887 USA (e-mail: igor.prikhodko@analog.com).

S. A. Zotov, A. A. Trusov, and A. M. Shkel are with the Department of Mechanical and Aerospace Engineering, MicroSystems Laboratory, University of California, Irvine, CA 92697 USA (e-mails: szotov@uci.edu; atrusov@uci.edu; ashkel@uci.edu).

Color versions of one or more of the figures in this paper are available online at http://ieeexplore.ieee.org.

Digital Object Identifier 10.1109/JMEMS.2013.2282936

and in-depth experimental study of gyrocompassing methods. Section 5 concludes the paper with a side-by-side analysis of carouseling and maytagging approaches.

II. Gyrocompassing Theory

The section reviews gyrocompassing principles, including carouseling and maytagging approaches.

A. Background

Gyrocompassing relies on inertial sensors to find the geographic direction, e.g. north or east, through the sensing of the Earth's rotation and gravity vector [15]. A horizontal angle between the observer and north direction is defined as azimuth, α, and measured from north in a clockwise direction, e.g. north is 0° and east is 90°. For such applications as land and aerial navigation, mining, or military, azimuth defines the horizontal direction of heading, pointing or targeting, respectively.

Desired azimuth accuracy, σ, in the range from 1 mrad to 4 mrad 50% probability error (PE) is often dictated by the mission requirement to achieve target location error, ϵ, in the range from 1 m to 4 m for each 1 km distance of travel, d [16]. The described calculation follows from the Abbe law (also known as sine error in dead reckoning), which describes the magnification of angular error (or heading) over distance:

$$\epsilon = d \sin \sigma.$$

While today's magnetic north finding solutions provide this level of resolution [17], the limitations of digital compasses due to magnetic field distortions make gyrocompassing (true north finding) an attractive alternative.

To find a horizontal angle (azimuth), the horizontal component of the Earth's rotation vector is measured by a gyroscope. The magnitude of the Earth's rotation rate, Ω_E, is constant, 15.041067 °/hr (roughly 0.0042 °/s), but its horizontal component, ω_h, depends on the latitude φ :

$$\omega_h = \Omega_E \cos \varphi. \tag{1}$$

For 33.7° N latitude in Irvine, CA, where all experiments were performed, the horizontal component of the Earth's rate is 12.5 °/hr. While for 71.4° N in Point Barrow, AK, the northernmost point of all U.S. territory, this component is only 4.8 °/hr. This magnitude is diminishing as the latitude approaches $\varphi = 90°$, complicating measurements in locations close to the North or South Pole (where all directions point north).

The azimuth angle α is detected by measuring a projection of the Earth's horizontal component onto a sensitive (input) axis of a gyroscope. To simplify experiments, the sensitive axis is kept parallel to the Earth surface so that all measurements are performed in a local tangential (horizontal) plane, also known as "east, north, up" geodetic plane, which is perpendicular to the gravity vector, Fig. 1. A vertically aligned gyroscope measures projection of the Earth's vector with a zero gravity effect on the output:

$$\omega = \omega_h \cos \alpha = \Omega_E \cos \varphi \cos \alpha. \tag{2}$$

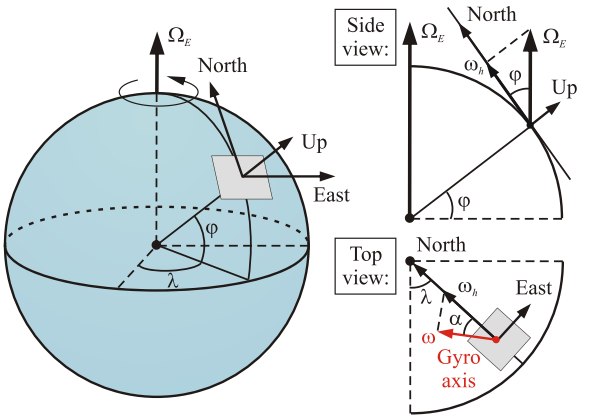

Fig. 1. Definition of azimuth, latitude, in a local horizontal ("east, north, up") plane for gyrocompassing applications.

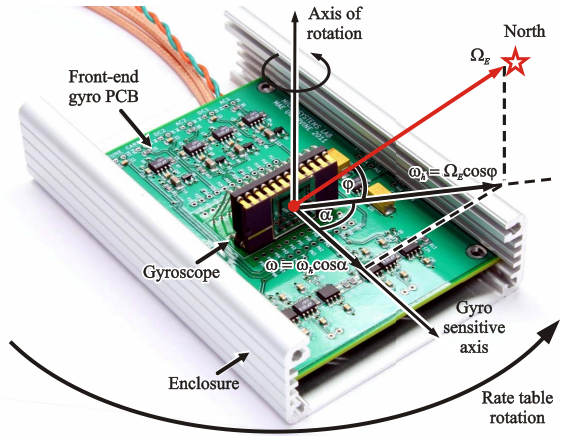

Fig. 2. Photo of the north-finding setup with a QMG rate sensor in a right angle DIP socket mounted on a rate table, with the axis of sensitivity parallel to the horizontal component of the Earth's rate vector.

Physical rotation of our setup around vertical (gravity) axis changes the horizontal orientation of the gyroscope's sensitive axis with respect to the north (Fig. 2), making possible determination of the azimuth angle (heading). Eq. (2) shows that the gyroscope aligned with the north direction ($\alpha = 0°$) measures maximal projection, ω_h, of the Earth's vector. In contrast, the output of the east pointing gyroscope ($\alpha = 90°$) is 0 °/hr. For this reason early gyrocompassing systems actually seek east because algorithmically it is more effective to find a null than a maximum peak [15], see Section III-A for detailed explanation. Such systems are aligned to east by rotating a gyroscope sensitive axis about local vertical axis until a zero output is sensed.

To determine the azimuth angle without performing physical rotation of a setup, two stationary gyroscopes with the orthogonal sensitive axes are often employed. Taking into account that $\cos(\alpha + 90°) = -\sin \alpha$, the output of these gyroscopes aligned with respect to the gravity is [18]:

$$\begin{aligned} \omega(0) &= \omega_h \cos \alpha, \\ \omega(90) &= -\omega_h \sin \alpha, \end{aligned} \tag{3}$$

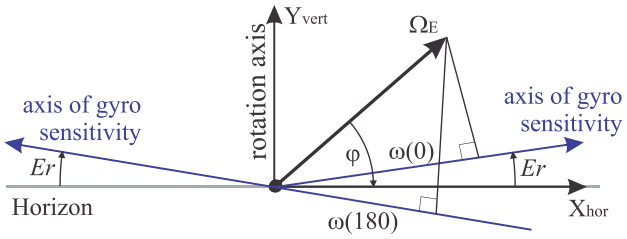

Fig. 3. Effect of the gyroscope misalignment with respect to the gravity, showing the projection of Earth's rotation axis on the gyroscope sensitive axis for the two-point azimuth measurement (at 0° and 180° turn table positions).

and used to instantaneously calculate the azimuth angle

$$\alpha = \arctan\left[-\frac{\omega(90)}{\omega(0)}\right]. \tag{4}$$

In practice, however, bias drifts of gyroscopes corrupt the measurements, thus calling for new approaches. Here, we investigate maytagging and carouseling approaches for bias drift mitigation using a z-axis MEMS Coriolis vibratory gyroscope.

B. Maytagging for North-Finding

"Maytagging" is an azimuth detection method accomplished by the $\pm 180°$ turning of the gyroscope sensitive axis. It is also commonly referred to as a two-point gyrocompassing [10] since it mitigates additive bias errors through the differential, two position azimuth measurement.

The system is initially set to an arbitrary azimuth angle α, and then rotated to 180° in either clockwise or counterclockwise direction. Taking into account that $\cos(\alpha + 180°) = -\cos\alpha$, the measurements of the gyroscope aligned to the local vertical level during maytagging are:

$$\begin{aligned}\omega(0) &= \omega_h \cos\alpha + b,\\ \omega(180) &= -\omega_h \cos\alpha + b,\end{aligned} \tag{5}$$

where ω_h is the Earth's rotation rate at a given latitude, α is the azimuth angle (heading), b is the gyroscope bias (null offset). The common bias error is observed by summing the measurements, Eq. (5), while the azimuth is recovered by subtracting the outputs:

$$\alpha = \arccos\left(\frac{\omega(0) - \omega(180)}{2\omega_h}\right). \tag{6}$$

In addition, the four-point azimuth measurement (or two position for a system of two orthogonal gyroscopes with different bias errors) allows to eliminate scale-factor errors as the term ω_h cancels out:

$$\alpha = \arctan\left[-\frac{\omega(90) - \omega(270)}{\omega(0) - \omega(180)}\right]. \tag{7}$$

The trade-off, however, is the increased sensitivity to bias drifts between the two orthogonal measurements, $\omega(90) - \omega(270)$ and $\omega(0) - \omega(180)$, as explained in Section III-A.

This method also algorithmically cancels out gravity errors due to misalignment of the gyroscope and alleviates the effect of cross-axis sensitivity, Fig. 3. Assuming the angle error Er between the sensitive axis of the gyroscope and the horizon, the outputs of the gyroscope at 0° and 180° turn table positions (with the speed of turn Ω) are:

$$\begin{aligned}\omega(0) &= \Omega_E \cos(\varphi - Er)\cos\alpha + \Omega \sin Er + b,\\ \omega(180) &= -\Omega_E \cos(\varphi + Er)\cos\alpha + \Omega \sin Er + b,\end{aligned} \tag{8}$$

resulting in the differential measurements:

$$\begin{aligned}\omega(0) + \omega(180) &= 2\Omega \sin Er + 2b,\\ \omega(0) - \omega(180) &= 2\Omega_E \cos\varphi \cos\alpha \cos Er.\end{aligned} \tag{9}$$

As follows from Eq. (9), the azimuth angle can be calculated from $\omega(0) - \omega(180)$, separately from the bias error and the effect of misalignment. At the same time, the bias errors due to gravity or misalignment can be identified from $\omega(0)+\omega(180)$. Taking into account the misalignment angle of 1° (or, alternatively, 0.9% cross-axis sensitivity), the measurement error at the latitude of Irvine, CA is given by:

$$2\omega_h(1-\cos Er) \approx 12.5\left(\frac{Er^2}{2} - \frac{Er^4}{24} + \cdots\right) = 0.004\ (°/\text{hr}),$$

which translates into less than 0.01 mrad error, surpassing the 4 mrad azimuth error requirement by two orders of magnitude.

C. Temperature Self-Compensation

The maytagging approach assumes constant gyroscope's bias during the two-point measurement. In practice, however, the angular rate measurements Eq. (5) cannot be performed simultaneously, resulting in bias variations between the measurements. One potential source of variations is susceptibility of the gyroscope to environmental temperature changes [11], [19]. For instance, the uncompensated temperature sensitivity on the order of 500 (°/hr)/°C is typical for MEMS [20], and presents a challenge for measurements of the Earth's rate (about 15 °/hr) in a variable temperature environment.

While conventional approaches for gyroscope's calibration rely on thermal models and external temperature sensors [11], we propose to utilize the resonant frequency as a measure of gyroscope's on-chip temperature. Similar to algorithms employed in a macroscale hemispherical resonator gyroscope [2], our approach takes advantage of temperature dependence of the drive-mode resonant frequency for self-compensation of temperature-induced drifts. The self-compensation algorithm is performed in real-time and inherently free from thermal lag or hysteresis. While we discussed temperature self-compensation in details in [19], [21], here we adopt the technique for maytagging measurements.

D. Carouseling for North-Finding

As an alternative to the two-point discrete azimuth measurement ("maytagging") and temperature self-compensation, the continuous modulation of the constant Earth's rate for separation from the bias drift is also possible. The continuous rotation, or "carouseling," of the platform allows identification of the azimuth angle independently of the bias and scale-factor errors (as long as the rate of rotation is faster than the low frequency drift of bias). Specifically, the platform rotation Ω causes a variation of angle between the Earth's rotation axis

and the gyroscope input axis (Fig. 2), leading to a modulation of a horizontal component ω_h and separation from bias b :

$$\omega(t) = \omega_h \cos(\Omega t + \alpha) + b.$$

The output is maximum when the gyroscope is pointing north, and minimum when it is pointing south. The sinusoidal fit to the gyroscope output is performed to extract the phase, which is a measure of heading. For each 360° turn, the azimuth angle α is calculated by subtracting a phase of the fit from instantaneous position of the turn table. At the same time, amplitude demodulation at the frequency of the applied rotation allows to extract time-varying bias and scale-factor independently of the azimuth (phase) measurements.

In contrast to maytagging mechanization, carouseling is more advantageous as it is robust to bias, scale-factor, and temperature drifts, although it requires a rotary platform with slip rings for continuous rotation. The key factor assuring insensitivity to these variations lies in a fact that the period of carouseling is faster than the time scale of bias drift (time constant of the bias instability point on Allan deviation plot), so that the only noise present in the gyroscope output is the angle random walk (or white noise). The trade-off is the additional measurement uncertainty due to the rate accuracy of a turn table (platform). Assuming a 0.01% typical accuracy and 1 °/s carouseling rate, the position error for each 360° turn is ±0.3 mrad, which is sufficient to perform azimuth measurements with the required 4 mrad uncertainty. Maytagging, on the other hand, can be implemented using a simple turn table, but requires temperature calibration, as discussed in Section II-C.

III. Noise Analysis and Sensor Requirements

In this section we analyze measurement errors and identify sensor requirements for achieving a single digit milliradian azimuth uncertainty.

A. Sensor Noise Requirements

The uncertainty of maytagging depends on the sensor bias drift between the two measurements. The uncompensated bias δb propagates to the differential azimuth measurement:

$$\frac{\omega(0) - \omega(180)}{2} = \omega_h \cos\alpha + \delta b, \tag{10}$$

and corrupts calculation, leading to an error, $\sigma(\alpha)$, between the true, α, and estimated azimuth [11]:

$$\sigma(\alpha) = \alpha - \arccos\left(\cos\alpha + \frac{\delta b}{\omega_h}\right) \approx \frac{\delta b}{\omega_h |\sin\alpha|}. \tag{11}$$

This equation suggests error reduction for angles $\alpha = \pm 90°$, $\pm 270°$. Thus, the measurements $\omega(90)$ and $\omega(270)$ are more precise than $\omega(0)$ and $\omega(180)$. In other words, the best precision is achieved by maytagging in the east-west direction as opposed to north-south.

Eq. (11) also reveals the sensitivity of azimuth measurement to the gyroscope bias. A similar expression can be derived for carouseling measurement. The upper bound for the error is:

$$\sigma(\alpha) \le \arctan\frac{\delta b}{\omega_h} \approx \frac{\delta b}{\Omega_E \cos\varphi}. \tag{12}$$

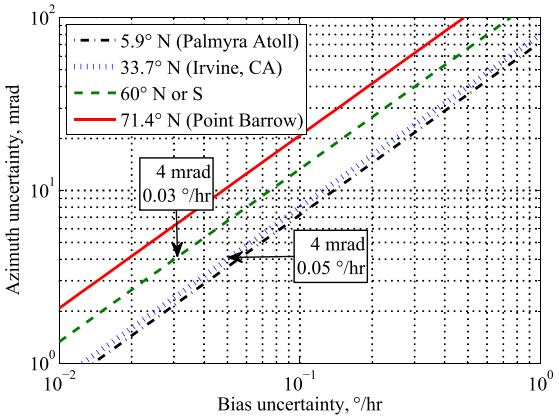

Fig. 4. Azimuth uncertainty as a function of a gyroscope bias at local latitude and extreme points of the US territory, demonstrating the sensor requirement of 0.03 °/hr to achieve 4 mrad error for latitude range from 60° S to 60° N.

Both Eqs. (11) and (12) show that the measurement uncertainty is the ratio of the gyroscope bias error to the horizontal component of the Earth's rate.

Fig. 4 shows the azimuth uncertainty $\sigma(\alpha)$ for $\alpha = \pm 90°$, as a function of gyroscope bias error δb and the latitude. As expected, uncertainty diminishes as the measurement location approaches to the equator (e.g., the southmost point of the US territory is 5.9° N at Palmyra Atoll). To achieve 4 mrad uncertainty from a single measurement, the sensor requirements is 0.05 °/hr bias error for the local latitude $\varphi = 33.7°$ N in Irvine, California, where experiments were performed. For most applications, the bias error metric is more strict and requires 0.03 °/hr as the latitude bounds are assumed to be between 60° S and 60° N [16] (e.g. the northmost point of the US territory is 71.4° N at Point Barrow, AK).

B. Sensor Structural Requirements

The operating principle of a vibratory z-axis angular rate gyroscope is based on energy transfer between two vibratory modes. The drive-mode, x-axis, is continuously excited at resonance, and the sense-mode, y-axis, is used for rate detection. The amplitude of the sense-mode (y) motion is proportional to the angular rate (Ω_z), with the angular gain factor ($0 < k \le 1$) and the drive amplitude (x) [22]:

$$y = 2Q_{\text{eff}} k \Omega_z x / \omega_y, \tag{13}$$

where ω_y is the sense-mode natural frequency. Here, Q_{eff} is the gain of the sense-mode at the drive-mode frequency ω_x:

$$Q_{\text{eff}} = Q_y / \sqrt{1 + 4Q_y^2(\Delta\omega/\omega_y)^2}, \tag{14}$$

which reaches the maximum Q_y at zero frequency mismatch between ω_x and ω_y, ($\Delta\omega = 0$).

It follows from Eq. (13) that the rate sensitivity is improved by maximizing the Q-factor, drive amplitude, angular gain, while reducing the resonant frequency and frequency mismatch. Q-factors above 100,000 have been previously realized for silicon MEMS gyroscopes, including the recently introduced quadruple mass gyroscope (QMG) [23]. The QMG

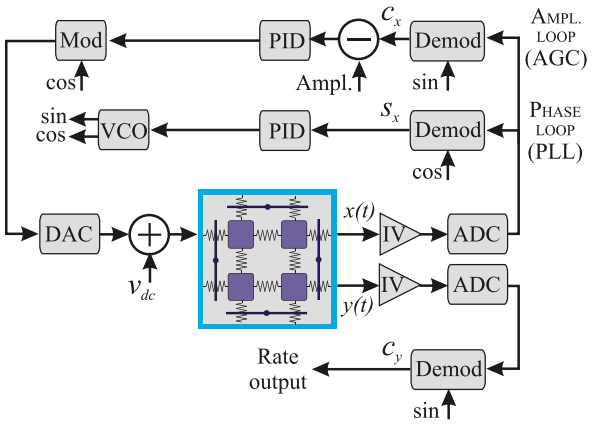

Fig. 5. Gyroscope control schematic, showing closed loop drive-mode and open loop sense-mode.

mechanical structure comprises four identical tines, four linear coupling flexures, and a pair of lever mechanisms for synchronization of the anti-phase drive- and sense-mode motion [24]. Momentum and torque balance in both x and y directions are expected to provide ultra-low dissipation of energy through the substrate, leading to a high resolution and equally high Q-factors, $Q_x = Q_y > 1$ million. The QMG architecture also provide high Coriolis coupling ($k \approx 1$), large amplitude of motion (several microns), and low operational frequency (2 kHz), which are essential for increasing the rate sensitivity.

Calculation of the fundamental mechanical-thermal noise limit for the QMG shows feasibility of achieving the required bias error metric (minimum detectable rotation rate). The model is based on the damped harmonic oscillator with the thermal noise having a Gaussian distribution and a bandwidth B. The rms rate equivalent noise (REN) of the mode-matched gyroscope (for the open-loop bandwidth $B = \omega_y/2Q_y$) due to this noise is given by [25]:

$$\Omega_{\text{REN}} = \frac{1}{2AQ_y}\sqrt{\frac{k_B T}{M}},$$

where k_B is the Boltzmann's constant, T is the temperature, M is the mass, A is the amplitude of the drive-mode motion, and Q_y is the sense-mode quality factor. For the following structural parameters of the QMG element $A = 2\cdot 10^{-6}$ m, $M = 1.7\cdot 10^{-6}$ kg, $Q = 10^6$, and $T = 300$ K, the predicted minimum detectable rate is on the order of 0.001 °/hr, sufficient for detecting azimuth with better than 4 mrad uncertainty.

C. Readout Electronics Requirements

The above error budget assumes only mechanical sensor noise, while for the estimation of overall noise the readout electronics should be also included. Fig. 5 shows block diagram of QMG signal processing for rate measurements, showing drive- and sense-mode control loops. For the angular rate measurements, the drive-mode was operated closed loop; the sense-mode remained open loop. A PLL drive loop sustained oscillation at resonance and provided reference for signals demodulation. An Automatic Gain Control (AGC) stabilized the amplitude of drive motion. Rotation was detected by demodulating the sense-mode signal. The rate measurements were performed at a 0.2 Hz separation between the drive- and the sense-mode frequencies.

Electrostatic actuation and capacitive detection were employed along with the electromechanical amplitude modulation (EAM) [26] for the parasitic feedthrough elimination. Instead of dc bias, the ac carrier voltage with 2.5 Vrms amplitude at 52 kHz frequency was applied to the mobile masses. The anchored differential sense-mode parallel-plate electrodes were connected to the inputs of a two-stage differential transimpedance amplification circuit implemented on a PCB, Fig. 2.

The output voltage noise of the transimpedance amplifier circuit is determined by the Johnson-Nyquist noise and the operational amplifier noise:

$$V_n = \sqrt{4k_B T R + e_n^2 + i_n^2 R^2},$$

where k_B is Boltzmann's constant, R is the feedback resistor value, T is the resistor's absolute temperature, e_n and i_n are the voltage and current noise densities of the amplifier, respectively. The Johnson noise for the $R = 10$ kΩ feedback resistor at a temperature of $T = 300$ K is $\sqrt{4k_B T R} = 13$ nV/$\sqrt{\text{Hz}}$. For the commercial off-the-shelf precision low noise and low input bias current operational amplifier (ADI OP1177), the values are $e_n = 8.5$ nV/$\sqrt{\text{Hz}}$ and $i_n = 0.2$ pA/$\sqrt{\text{Hz}}$. The resulting output noise of operational amplifier is $\sqrt{e_n^2 + i_n^2 R^2} = 9$ nV/$\sqrt{\text{Hz}}$, which is comparable to the Johnson noise. The total thermo-electrical noise is $V_n = 16$ nV/$\sqrt{\text{Hz}}$.

The rate equivalent noise can be calculated using a scale-factor conversion. The gyroscope scale-factor is determined by the pick-off scheme and by the gyroscope dynamics:

$$\text{SF} = \text{SF}_{\text{elec}} \cdot \text{SF}_{\text{mech}},$$

where SF_{elec} is the pick-off electronics scale-factor in V/m units, and SF_{mech} is the scale-factor calculated from sensor dynamics in m/(°/hr) units. The proof-mass motion modulates the pick-off capacitor gap and generates the current, which is converted to the voltage with the transimpedance gain R proportional to [26]:

$$|V| = \frac{1}{2} R \frac{C_{\text{sn}}}{d} v_c(\omega_c - \omega_d)|x| = \text{SF}_{\text{elec}}|y|,$$

where C_{sn} is a nominal capacitance of the sense-mode pick-off electrodes, d is the capacitor nominal gap, v_c is the ac carrier voltage, ω_c is the carrier frequency, ω_d is the drive frequency, and $|y|$ is the amplitude of motion. The estimated scale-factor is $\text{SF}_{\text{elec}} = 1.56$ mV/μm for values $C_{\text{sn}} = 2$ pF, $d = 5$ μm, $v_c = 2.5$ V, $\omega_c = 2\cdot\pi\cdot 52$ kHz, and $\omega_d = 2\cdot\pi\cdot 2.2$ kHz.

The scale-factor SF_{mech} can be estimated from Eqs. (13) and (14). According to Eq. (14), the effective quality factor decreases to the value of 5500 for the mismatch of $\Delta\omega = 2\cdot\pi\cdot 0.2$ Hz and the sense-mode frequency of $\omega_y = 2\cdot\pi\cdot 2.2$ kHz. Taking into account the angular gain factor $k = 0.87$ and the drive-mode amplitude of $|x| = 2$ μm,

the resulting scale-factor is $SF_{mech} = 1.4\ \mu m/(rad/s)$, or 6.7 pm/(°/hr).

Finally, the scale-factor is

$$SF = 1.56\ mV/\mu m \cdot 6.7\ pm/(°/hr) = 10\ nV/(°/hr),$$

and the rate equivalent noise due to electronics is

$$\Omega_{REN} = \frac{V_n}{SF} = \frac{16\ nV/\sqrt{Hz}}{10\ nV/(°/hr)} = 1.6\ (°/hr)/\sqrt{Hz}.$$

Although electronics noise could limit the measurement time of azimuth, the QMG mechanical structure has potential for reaching 10^{-3} (°/hr)/$\sqrt{Hz}$ [27], suggesting that the overall noise can be improved by the optimal electronics design. For instance, the gain of transimpedence amplifier can be further optimized by increasing the feedback resistance. Nevertheless, the current value of 10 kΩ ensures the phase shift of below few degrees at the carrier frequency of 52 kHz (assuming a stray capacitance of 1 pF), providing the effective separation of the rate signal from the quadrature error [28].

IV. Experimental Results

A north-finding setup consisting of a QMG sensor, front-end PCB, and a rate table is shown in Fig. 2. A stand-alone QMG was fabricated using an in-house SOI process and vacuum sealed using the ceramic package level technology. The QMG sensor was mounted on a PCB with front-end amplifiers and installed on the 1291 Ideal Aerosmith rate table enclosed in a thermal chamber. All reported experiments were carried out using a custom PCB connected to a HF2 digital lock-in amplifier from the Zurich Instruments (ZI), providing control and signal conditioning for the QMG. The North direction was detected by changing the orientation of the gyroscope z-axis relative to the Earth's rotation vector. The horizontal component was observed after orienting the QMG sensitive axis parallel to the local vertical plane, as shown in Fig. 2. A rate table was used to position the gyroscope in the local horizontal plane.

A. Sensor Characterization

The mechanical characterization of the 2 kHz QMG sensor was performed by ring-down tests, which revealed drive- and sense-mode Q-factors of 1.17 million with a relative damping mismatch ΔQ/Q of 1% [13]. Thermal cycling demonstrated Q-factors of 0.7 million for temperatures up to 100 C [13]. The frequency symmetry evaluated in [23] confirmed closely matched temperature coefficients of frequency (TCF) in a wide temperature range with a 0.2 ppm/C uncertainty.

The low dissipation QMG sensor demonstrated low noise characteristics. The Allan deviation plot of a zero rate output recorded for 2 hours is shown in Fig. 6. For relatively short averaging time the QMG output is dominated by the angle random walk of 0.07 °/$\sqrt{hr}$, in a fairly good agreement with the predicted noise due to electronics, 1.6 (°/hr)/$\sqrt{Hz}$ = 0.03 °/$\sqrt{hr}$. The difference is partially attributed to additional noise sources such as an A/D converter and a scaling amplifier employed in the lock-in amplifier. The bias instability reaches a value of 0.2 °/hr for 10 min of averaging. For longer integration, a slope of τ^{+1} is observed, which is attributed to the temperature ramp.

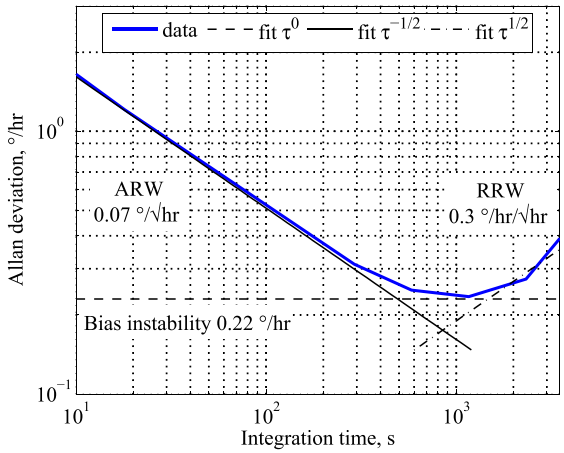

Fig. 6. Measured Allan deviation of the QMG rate sensor, revealing a 0.07 °/$\sqrt{}$hr ARW, and a 0.22 °/hr bias instability.

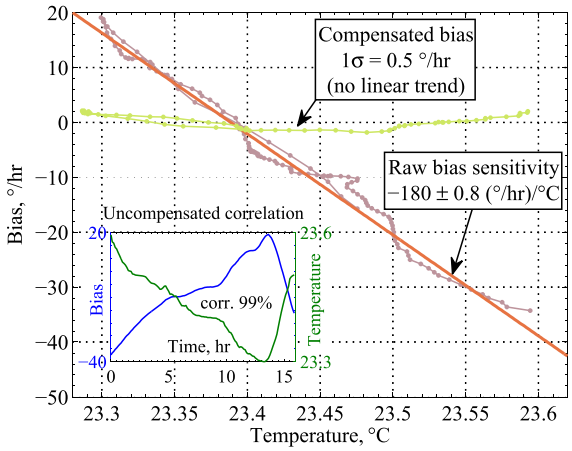

Fig. 7. QMG thermal dependence. The uncompensated bias sensitivity is −180 (°/hr)/C; self-calibration removes a linear trend. Inset: bias and temperature correlation.

Characterization of bias temperature sensitivity revealed the uncompensated value of −180 (°/hr)/°C, Fig. 7, attributed to the packaging stresses in early QMG prototypes. The temperature self-compensation using the drive-mode frequency as thermometer, [19], removed a linear sensitivity of the null offset (bias) to below 0.5 °/hr uncertainty, Fig. 7, attesting feasibility of the long-term stable measurements required for the north-finding.

B. Characterization of Gyrocompassing Setup

Characterization of the experimental setup is crucial for understanding the repeatability and accuracy of maytagging and carouseling measurements. An optical characterization method was developed to precisely measure the azimuth uncertainty of the setup [29], Fig. 2. The method relies on measuring a misalignment of the gyroscope fixture before and after each 360° full turn.

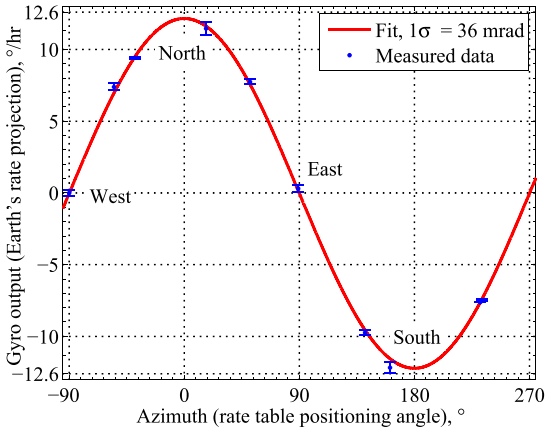

Fig. 8. Measured projection of the Earth's rate as function of azimuth using the differential maytagging approach. Gyro output is 12.5 °/hr (Irvine, CA) when pointing North.

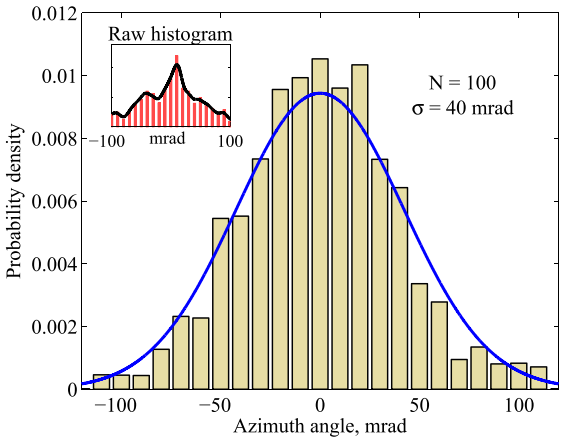

Fig. 9. East-west azimuth histogram with normal distribution fit after temperature self-compensation, showing a 40 mrad error. Inset: raw histogram.

The gyroscope fixture is rotated using a precision-controlled single-axis Ideal Aerosmith 1291BR rate table with an angular accuracy of ± 0.07 mrad and repeatability of ± 0.015 mrad. At the same time, reflection of a collimated laser beam from the sensor's glass lid is observed using a calibrated detection screen at a 1.5 m distance. The following procedure is used to obtain misalignment data from the sensor's package before and after each rate table turn:

1) Mark the position of the laser beam reflected off of sidewall. This acts as a reference for later measurements.
2) Precisely rotate the gyroscope by 360° and mark the position of the laser beam reflected off of the glass lid.
3) Measure the distance between the two reference marks from the glass lid and multiply by the calibrated sensitivity of the detection grid to calculate misalignment ($1° = 17.4$ mrad).
4) Repeat Step 2 and 3 for statistical data analysis.
5) Change the rate table speed and Repeat Step 2 and 3.

Results of all alignment stability tests on accuracy and precision of the gyrocompassing setup suggest that the overall accuracy of the setup is ± 0.2 mrad, while the precision defined by the rate table positioning repeatability is ± 0.07 mrad. The lower limit of detection of the optical measurement setup defined by the laser spot size (1 mm) is approximately ± 0.18 mrad, therefore the misalignment of the setup is likely much lower than the measured data. These results indicate feasibility of the azimuth measurements with an uncertainty sufficiently better than 4 mrad.

C. North-Finding by Maytagging

This section presents 2-point gyrocompassing results. Fig. 8 shows the horizontal component of the Earth's rotation vector as a function of positioning angle. Each datapoint is produced by changing the rate table positioning angle and taking a two-point differential measurement of the QMG output according to Eq. (10). The measurement time was determined by the time necessary to reach the bias instability, ensuring that the only dominant noise on this timescale is the angle random walk (white noise with slope $\tau^{-1/2}$). According to Fig. 6, the minimum Allan deviation of 0.2 °/hr occurs after 10 min, allowing for 5 min averaging time at each position. As shown in Section III-A, maytagging in the east-west direction minimizes propagation of errors because the slope at these locations is linear rather than infinite (vertical line) at the north-east locations, Fig. 8. Although the sinusoidal fit is not typically employed for maytagging measurements, we only use it to roughly estimate the east/west location and perform all experiments at this location. The sinusoid amplitude was 12.5 °/hr, in good agreement with the Earth's rate component at 33.7° N latitude (Irvine, CA).

The maytagging performance was measured by statistical analysis. The classical estimation of azimuth error, Eq. (12), suggested a 0.05 °/hr bias instability requirement to achieve 4 mrad precision from a single measurement. Although we demonstrate only 0.2 °/hr Allan deviation bias instability for our current QMG sensor, the same 4 mrad uncertainty can be reached by filtration of multiple azimuth datapoints. The filtering, however, requires a stationary normal distribution of errors and increase in the north-finding time. To evaluate the distribution of noise we collected 100 multiple-turn datapoints. The east-west direction was chosen to minimize error propagation. Azimuth probability density histograms of raw and temperature self-compensated data is shown in Fig. 9. The fit to normal distribution curve revealed a Gaussian error model for compensated data. The self-compensation removed temperature-induced bias drifts between the two-point measurement, yielding a normal distribution of random errors, Fig. 9. Filtration diminished uncertainty with a 44 mrad/$\sqrt{\mathrm{N}}$ slope, providing a 4.4 mrad precision after $\mathrm{N} = 100$ averages, Fig. 10.

D. North-Finding by Carouseling

In this section we evaluate the carouseling approach for the bias compensated north-finding. In contrast to the discrete $\pm 180°$ maytagging, the carouseling requires continuous rotation of the gyroscope sensitive axis. The technique relies on

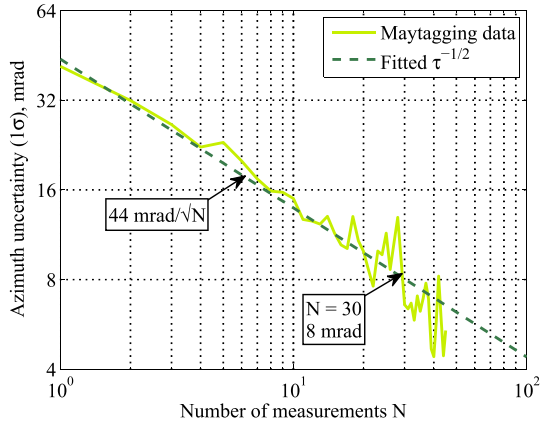

Fig. 10. Maytagging azimuth error (1-σ) as a function of number of filtered measurements using Fig. 9 data. Error scales down as 44 mrad/$\sqrt{N}$, resulting in 4.4 mrad after N = 100.

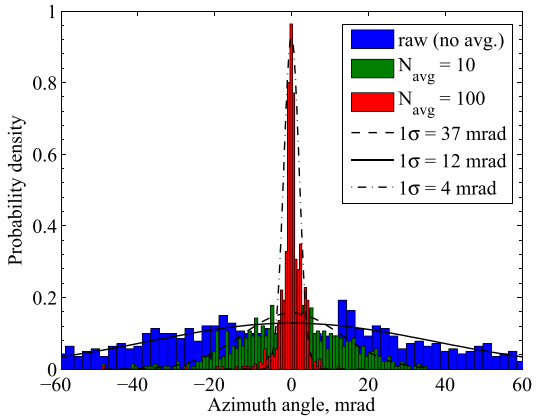

Fig. 12. Histogram of 400 azimuth datapoints with normal distribution fits obtained by carouseling, showing convergence of error from 37 to 4 mrad.

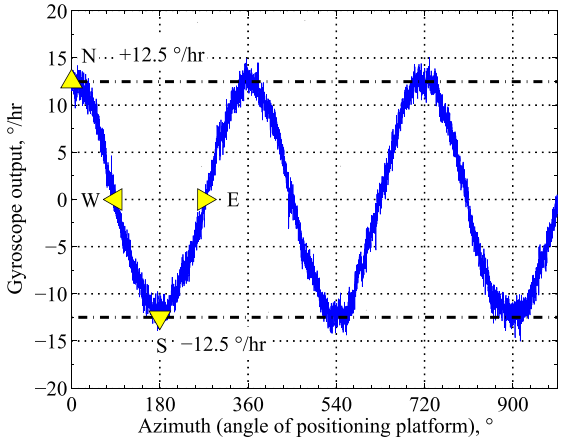

Fig. 11. QMG output produced by the Earth's rotation (12.5 °/hr at 33.7° N latitude) during carouseling shown as a function of rate table angular position.

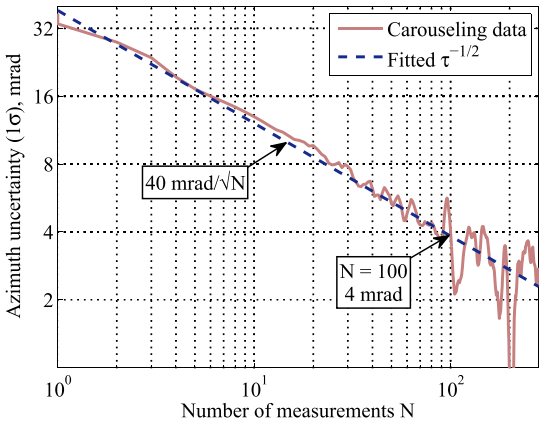

Fig. 13. Azimuth uncertainty as a function of number of filtered measurements from Fig. 12 data. A 4 mrad uncertainty is achieved by filtering of N = 100 points.

amplitude modulation of the constant Earth's rate to separate bias and scale factor drifts, as well as other temperature-dependent errors.

The QMG sensor mounted on a rate table was rotated in a horizontal plane defined by the rate table with 1 °/s angular rate. This resulted in a periodic rotation of the QMG sensitive axis and modulation of the Earth's constant rate with a 6 min period. Fig. 11 shows a QMG output from a carouseling run. As expected, the sinusoidal variation was maximum, 12.5 °/hr, pointing north, and minimum, −12.5 °/hr, pointing south.

The carouseling precision was measured by the statistical analysis. Every 6 min azimuth was extracted in real-time from a sinusoidal fit. Each period (each 360° turn) the data was logged and a sinusoidal fit was performed in real-time to obtain the azimuth angle and other parameters (during which the temperature is assumed to be constant). Every period a new set of azimuth, bias, and scale-factor was obtained and analyzed. The gyroscope bias was extracted from the offset value of the fit, the scale-factor was recovered from the amplitude of the fit, and, finally, the azimuth angle was determined from the phase of the fit. The chosen period of rotation (6 min) roughly corresponds to the timescale where the only noise process present in the gyroscope output is white (from 10 s to 360 s, see the slope $\tau^{-1/2}$ in the Allan deviation Fig. 6), as opposed to the timescale of low-frequency drift processes such as rate random walk $\tau^{1/2}$ or temperature ramp τ^{1} (from 10^3 s and up), which cannot be averaged or effectively eliminated.

The demodulation process (fit) removed the low-frequency drift of the bias (as well as the scale-factor) due to room temperature fluctuations, as shown in Fig. 7 inset. Specifically, azimuth was calculated by taking the difference between the phase of a sinusoidal fit and instantaneous angular position of the rate table. Fig. 12 shows a histogram of 400 raw and averaged azimuth angles. The carouseling approach was proved to be robust to scale-factor, bias and temperature variations despite the sensitivity of –180 (°/hr)/°C (Fig. 7), thus yielding a normal distribution of errors without any temperature calibration (as previously required for maytagging). This allowed reducing uncertainty by the data averaging. Normal distribution fits in Fig. 12 demonstrate convergence of standard deviation as a number of averages. Similar to maytagging, the uncertainty scaled down as 40 mrad/$\sqrt{N}$. A 4 mrad uncertainty was reached by filtering of N = 100 points, Fig. 13.

V. Discussions

The further improvement in azimuth uncertainty is possible by optimizing the readout electronics noise, selecting the transimpedance amplifier with the low input referred current noise density while preserving the low input capacitance, as well as by increasing the feedback gain without adversely affecting the phase relationship between the sensor signals, as outlined in Section III-C. The improvement in total measurement time is possible by increasing the carouseling rotation rate up to the gyroscope bandwidth limit. While in the current work the open-loop gyroscope bandwidth has limited the carouseling rate to below 1 °/s, the closed-loop or force-to-rebalance operation [22] is envisioned to improve the bandwidth significantly, without adversely affecting the gyroscope noise.

In this work, a comparative analysis of MEMS gyrocompassing methods was done using a rate table. To enable a truly compact MEMS gyrocompass, the development of MEMS gimbals [16], [30] or rotary stages [31], [32] is, thus, critical. Alternative approaches eliminating a need for physical rotation of a gyroscope include bias/scale-factor self-calibration [33], [34], and virtual carouseling (without a rate table) [8].

VI. Conclusion

We demonstrated north-finding with 4 mrad precision using a silicon MEMS quadruple mass gyroscope with 0.2 °/hr bias instability and 1.2 million Q-factor in the drive and sense directions. Carouseling and maytagging methods were implemented for true north detection using the Earth's rotation. Both methods produced an azimuth estimation with uncertainty diminishing as the square root of the number N of turns, $\sigma(\mathrm{N}) = 40\ \mathrm{mrad}/\sqrt{\mathrm{N}}$. The carouseling was robust to bias and scale factor changes despite the temperature drift of -180 (°/hr)/°C (attributed to packaging stresses), but required the precise continuous rotation. In contrast, the maytagging relied on discreet 180° turns, but required the temperature calibration. It is hypothesized that the reduction of maytagging averaging time could potentially eliminate the need for temperature calibration since temperature drifts would not be present at shorter timescales, although an azimuth uncertainty could be adversely affected (less amount of data for averaging).

The reported results clearly show feasibility of silicon inertial MEMS for precision north-finding, currently limited to high resolution macroscale gyroscopes or magnetic compasses. The ongoing work on the on-chip interconnects and electronics is expected to reduce north-finding time from several hours down to a minute by optimizing the front-end electronics noise and improving the gyroscope bandwidth.

Acknowledgment

The authors would like to acknowledge Dr. Flavio Heer from Zurich Instruments AG and Ilya Chepurko from Mistras Group, Inc for assistance with the electronics and Dr. Burgess Johnson from Honeywell Aerospace for insightful comments. The gyroscopes were designed and characterized at the MicroSystems Laboratory, University of California, Irvine.

References

[1] A. Shkel, "Microtechnology comes of age," *GPS World*, vol. 22, pp. 43–50, Sep. 2011.

[2] D. M. Rozelle, "The hemispherical resonator gyro: From wineglass to the planets (AAS 09-176)," in *Proc. 19th AAS/AIAA Space Flight Mech. Meeting*, Feb. 2009, pp. 1157–1178.

[3] P. B. Ruffin, "Progress in the development of gyroscopes for use in tactical weapon systems," in *Proc. 7th Annu. Int. Symp. Smart Struct. Mater.*, 2000, pp. 2–12.

[4] P. B. Ruffin, J. G. Sawyer, C. C. Sung, and J. Bush, "Progress in miniaturizing fiber optic gyroscope components for tactical weapon systems," in *Proc. Int. Symp. Opt. Sci., Eng. Instrum.*, 1996, pp. 345–355.

[5] F. Ayazi, "Multi-DOF inertial MEMS: From gaming to dead reckoning," in *Proc. 16th Int. Conf. Solid-State Sensors, Actuators Microsyst.*, Jun. 2011, pp. 2805–2808.

[6] B. Johnson, E. Cabuz, H. French, and R. Supino, "Development of a MEMS gyroscope for northfinding applications," in *Proc. IEEE/ION Position, Location Navigat. Symp.*, May 2010, pp. 168–170.

[7] W. Geiger et al., "MEMS IMU for AHRS applications," in *Proc. IEEE/ION Position, Location Navigat. Symp.*, May 2008, pp. 225–231.

[8] K. Shcheglov, S. Orlov, J. Ha, and K. Ezal, "Breakthrough and challenges of C-SWAP technology development," in *Proc. JSDE/ION JNC*, Jun. 2012, pp. 1–10.

[9] M. Zaman, A. Sharma, Z. Hao, and F. Ayazi, "A mode-matched silicon-yaw tuning-fork gyroscope with subdegree-per-hour Allan deviation bias instability," *J. Microelectromech. Syst.*, vol. 17, no. 6, pp. 1526–1536, Dec. 2008.

[10] R. Arnaudov and Y. Angelov, "Earth rotation measurement with micromechanical yaw-rate gyro," *IOP Meas. Sci. Technol.*, vol. 16, no. 11, pp. 2300–2303, 2005.

[11] L. I. Iozan, M. Kirkko-Jaakkola, J. Collin, J. Takala, and C. Rusu, "Using a MEMS gyroscope to measure the Earth's rotation for gyrocompassing applications," *Meas. Sci. Technol.*, vol. 23, no. 2, pp. 025005-1–025005-3, 2012.

[12] A. Trusov, I. Prikhodko, S. Zotov, and A. Shkel, "High-Q and wide dynamic range inertial MEMS for north-finding and tracking applications," in *Proc. IEEE/ION PLANS*, Apr. 2012, pp. 247–251.

[13] I. Prikhodko, S. Zotov, A. Trusov, and A. Shkel, "Sub-degree-per-hour silicon MEMS rate sensor with 1 million Q-factor," in *Proc. 16th Int. Conf. Solid-State Sensors, Actuators Microsyst.*, Jun. 2011, pp. 2809–2812.

[14] I. Prikhodko, A. Trusov, and A. Shkel, "North-finding with 0.004 radian precision using a silicon MEMS quadruple mass gyroscope with Q-factor of 1 million," in *Proc. IEEE Int. Conf. Micro-Electro-Mech. Syst.*, Jan. 2012, pp. 164–167.

[15] A. Lawrence, *Modern Inertial Technology*. New York, NY, USA: Springer-Verlag, 1998.

[16] J. Pritchett, C. Lange, and J. Warren, "System design trades in gimbaled MEMS northfinding systems," in *Proc. JSDE/ION JNC*, Jun. 2012, pp. 25–30.

[17] (Aug. 2006). *Datasheet for Honeywell μpoint HMR3600 Digital Magnetic Compass* [Online]. Available: http://www51.honeywell.com/aero/common/documents/myaerospacecatalog-documents/Defense_Brochures-documents/Honeywell_Magnetic_Sensors_and_Compassing_Solutions.pdf

[18] A. Meyer and D. Rozelle, "Milli-HRG inertial navigation system," in *Proc. IEEE/ION PLANS*, Apr. 2012, pp. 24–29.

[19] I. Prikhodko, A. Trusov, S. Zotov, and A. Shkel, "Achieving long-term bias stability in high-Q inertial MEMS by temperature self-sensing with a 0.5 millicelcius precision," in *Proc. Solid-State Sensors, Actuators, Microsyst. Workshop*, Jul. 2012, pp. 287–290.

[20] M. Weinberg and A. Kourepenis, "Error sources in in-plane silicon tuning-fork MEMS gyroscopes," *J. Microelectromech. Syst.*, vol. 15, no. 3, pp. 479–491, Jun. 2006.

[21] I. P. Prikhodko, A. A. Trusov, and A. M. Shkel, "Compensation of drifts in high-Q MEMS gyroscopes using temperature self-sensing," *Sens. Actuators A, Phys.*, vol. 201, pp. 517–524, Oct. 2013.

[22] D. Lynch, "Coriolis vibratory Gyros," in *Proc. Symp. Gyro Technol.*, 1998, pp. 1.0–1.14.

[23] A. Trusov, I. Prikhodko, S. Zotov, and A. Shkel, "Low-dissipation silicon tuning fork gyroscopes for rate and whole angle measurements," *IEEE Sensors J.*, vol. 11, no. 11, pp. 2763–2770, Nov. 2011.

[24] A. A. Trusov, A. R. Schofield, and A. M. Shkel, "Micromachined tuning fork gyroscopes with ultra-high sensitivity and shock rejection," U.S. Patent 20 100 313 657, Dec. 16, 2010.

[25] R. Leland, "Mechanical-thermal noise in MEMS gyroscopes," *IEEE Sensors J.*, vol. 5, no. 3, pp. 493–500, Jun. 2005.
[26] A. Trusov and A. Shkel, "A novel capacitive detection scheme with inherent self-calibration," *J. Microelectromech. Syst.*, vol. 16, no. 6, pp. 1324–1333, Dec. 2007.
[27] A. A. Trusov, A. R. Schofield, and A. M. Shkel, "Micromachined rate gyroscope architecture with ultra-high quality factor and improved mode ordering," *Sens. Actuators A, Phys.*, vol. 165, no. 1, pp. 26–34, 2011.
[28] A. Sharma, "CMOS systems and circuits for sub-degree per hour MEMS gyroscopes," Ph.D. dissertation, Georgia Institute of Technol., Atlanta, GA, USA, 2007.
[29] S. Zotov, M. Rivers, A. Trusov, and A. Shkel, "Folded MEMS pyramid inertial measurement unit," *IEEE Sensors J.*, vol. 11, no. 11, pp. 2780–2789, Nov. 2011.
[30] S. Mohiuddin, M. McManus, P. Sherman, R. Elliot, M. Little, and S. Holmes, "Gimbaled MEMS IMU techniques in inertial navigation," in *Proc. JSDE/ION JNC*, Jun. 2012, pp. 1–8.
[31] B. Yoxall, M.-L. Chan, R. Harake, T. Pan, and D. Horsley, "Rotary liquid droplet microbearing," *J. Microelectromech. Syst.*, vol. 21, no. 3, pp. 721–729, Jun. 2012.
[32] E. E. Aktakka, R. L. Peterson, and K. Najafi, "A 3-DOF piezoelectric micro vibratory stage based on bulk-PZT/silicon crab-leg suspensions," in *Proc. 6th IEEE Int. Conf. MEMS*, Jan. 2013, pp. 576–579.
[33] M. H. Kline, Y. C. Yeh, B. Eminoglu, I. I. Izyumin, M. Daneman, D. A. Horsley, and B. E. Boser, "MEMS gyroscope bias drift cancellation using continuous-time mode reversal," in *Proc. Solid-State Sensors, Actuators Microsyst. Conf.*, Jun. 2013, pp. 1–15.
[34] A. Trusov, I. Prikhodko, D. Rozelle, and A. Shkel, "1 ppm precision self-calibration of scale factor in MEMS Coriolis vibratory gyroscopes," in *Proc. Solid-State Sensors, Actuators Microsyst. Conf.*, Jun. 2013, pp. 2531–2534.

Igor P. Prikhodko (S'09–M'13) is a MEMS Advanced Development Engineer with Analog Devices, Inc., in the greater Boston area, where he focuses on R&D of advanced inertial MEMS sensors. He received the B.S. degree in mechanics and mathematics from Moscow State University, Moscow, Russia, in 2007, and the M.S. and Ph.D. degrees in mechanical and aerospace engineering from the University of California, Irvine, CA, USA, in 2008 and 2013, respectively. His work is published in over 25 peer-reviewed journal and refereed conference papers. Dr. Prikhodko is a recipient of the Outstanding Paper Award at Transducers 2011 and the Best Paper Award at IMAPS Device Packaging 2012 conferences. He serves as a reviewer for major MEMS journals and on program committees for the IEEE International Symposium on Inertial Sensors and Systems and the International Symposium on Microelectronics. He is a member of the American Society of Mechanical Engineers.

Sergei A. Zotov (M'11) received the M.S. and Ph.D. degrees in mechanical engineering and control systems from Tula State University, Tula, Russia, in 1999 and 2002, respectively. He is currently a Post-Doctoral Scientist with the MicroSystems Laboratory, University of California, Irvine, CA, USA, where he is responsible for the development, design, fabrication, and testing of micromachined devices and systems for inertial navigation. Over the last 12 years, his focus has been on the Research and Development of MEMS gyroscopes and accelerometers. He has published seven journal and 16 international conference papers in the field of inertial MEMS. He holds eight Russian patents, one U.S. patent, and three U.S. patents pending. Dr. Zotov is a recipient of the Gold Medal at the International Salon of Inventions 2004 in Geneva, Switzerland, and the Outstanding Paper Award at the Transducers 2011 and the Best Paper Award at IMAPS Device Packaging 2012 conferences. Dr. Zotov is a reviewer for major MEMS journals.

Alexander A. Trusov (S'06–M'09) is a Senior Research Scientist with Northrop Grumman Corporation, where he focuses on R&D of advanced navigation sensors and instruments. Dr. Trusov received the B.S. and M.S. degrees in applied mathematics and mechanics from Moscow State University, Moscow, Russia, in 2004, and the M.S. and Ph.D. degrees in mechanical and aerospace engineering from the University of California, Irvine (UCI), CA, USA, in 2006 and 2009, respectively. From 2009 to 2013, he was a Project Scientist in the Mechanical and Aerospace Department at UCI. While at UCI, he served as the PI and a co-PI on more than half a dozen of DoD sponsored projects. Dr. Trusov's research interests include design, modeling, fabrication, and vacuum packaging of micromachined inertial systems, sensor and instrument self-calibration, design of characterization experiments, and statistical data processing and analysis. Dr. Trusov has published over 60 journal and conference papers has four issued U.S. patents (half a dozen more pending) on these topics. He is a recipient of the Outstanding Paper Award at Transducers 2011, the Design Contest Award at System-on-Chip Conference 2011, and the Best Paper Award at IMAPS Device Packaging Conference 2012. Dr. Trusov serves on program committees for the Saint Petersburg International Conference on Integrated Navigation Systems, the IEEE International Symposium on Inertial Sensors and Systems, and the IEEE/ION Position Location and Navigation Symposium. He is a member of the American Society of Mechanical Engineers and the Institute of Navigation.

Andrei M. Shkel (S'95–A'98–SM'08) is a Professor in the Department of Mechanical and Aerospace Engineering, University of California, Irvine, CA, USA. From 2009 to 2013, Dr. Shkel served as a Program Manager in the Microsystems Technology Office, Defense Advanced Research Projects Agency (DARPA), Arlington, VA, USA, where he created and managed a comprehensive portfolio of programs focused on microtechnology for positioning, navigation, and timing applications. His professional interests reflected in over 160 publications and two books, including solidstate sensors and actuators, MEMS-based neuroprosthetics, sensor-based intelligence, and control theory. He holds 21 U.S. and worldwide patents (12 are pending) on micromachined angle-measuring gyroscopes, wide-bandwidth rate gyroscopes, design and fabrication of light manipulators and tunable optical filters, and hybrid micromachining processes. Dr. Shkel has served on a number of editorial boards, most recently as an Editor of the JOURNAL OF MICROELECTROMECHANICAL SYSTEMS, a member of editorial board for the *International Journal on Smart Structures and Systems*, a TPC member of Hilton Head 2009, and a general chair of the 2005 IEEE Sensors Conference. He has been awarded the IEEE Sensors Council 2009 Technical Achievement Award, the 2005 NSF CAREER Award, the 2002 George E. Brown, Jr. Award, and the 2006 Best Faculty Research Award. In 2013, he received the Office of the Secretary of Defense Medal for Exceptional Public Service for his work at DARPA as a Program Manager. Dr. Shkel received the Diploma in mechanics and mathematics from Moscow State University, Moscow, Russia, in 1991, and the Ph.D. degree in mechanical engineering from the University of Wisconsin at Madison, Madison, WI, USA, in 1997.